

# Accelerator-Based Biological Irradiation Facility Simulating Neutron Exposure from an Improvised Nuclear Device

Yanping Xu,<sup>a,1</sup> Gerhard Randers-Pehrson,<sup>a</sup> Helen C. Turner,<sup>b</sup> Stephen A. Marino,<sup>a</sup> Charles R. Geard,<sup>a</sup> David J. Brenner<sup>b</sup> and Guy Garty<sup>a,2</sup>

<sup>a</sup> Radiological Research Accelerator Facility, Columbia University, Irvington, New York 10533 and <sup>b</sup> Center for Radiological Research, Columbia University, New York, New York 10032

---

Xu, Y., Randers-Pehrson, G., Turner, H. C., Marino, S. A., Geard, C. R., Brenner, D. J. and Garty, G. Accelerator-Based Biological Irradiation Facility Simulating Neutron Exposure from an Improvised Nuclear Device. *Radiat. Res.* 184, 404–410 (2015).

We describe here an accelerator-based neutron irradiation facility, intended to expose blood or small animals to neutron fields mimicking those from an improvised nuclear device at relevant distances from the epicenter. Neutrons are generated by a mixed proton/deuteron beam on a thick beryllium target, generating a broad spectrum of neutron energies that match those estimated for the Hiroshima bomb at 1.5 km from ground zero. This spectrum, dominated by neutron energies between 0.2 and 9 MeV, is significantly different from the standard reactor fission spectrum, as the initial bomb spectrum changes when the neutrons are transported through air. The neutron and gamma dose rates were measured using a custom tissue-equivalent gas ionization chamber and a compensated Geiger-Mueller dosimeter, respectively. Neutron spectra were evaluated by unfolding measurements using a proton-recoil proportional counter and a liquid scintillator detector. As an illustration of the potential use of this facility we present micronucleus yields in single divided, cytokinesis-blocked human peripheral lymphocytes up to 1.5 Gy demonstrating 3- to 5-fold enhancement over equivalent X-ray doses. This facility is currently in routine use, irradiating both mice and human blood samples for evaluation of neutron-specific biodosimetry assays. Future studies will focus on dose reconstruction in realistic mixed neutron/photon fields. © 2015 by Radiation Research Society

---

## OVERVIEW

Several scenarios of large-scale radiological events include the use of an improvised nuclear device (IND) that may produce a significant neutron component with prompt

radiation exposure (1). Specifically, the prompt radiation from this type of detonation is expected to be qualitatively similar to that of the gun-type 15 kT device exploded over Hiroshima (2). To assess the significance of the neutron exposure in dose reconstruction for this type of scenario, and to allow characterization of novel neutron-specific biodosimetry assays, a new broad-energy neutron irradiator was designed at the Columbia University Radiological Research Accelerator Facility (RARAF) (3).

This accelerator-driven neutron irradiator provides a broad-spectrum neutron field with energies from 0.2 to 9 MeV that mimics the evaluated energy spectrum produced in the detonation of the atomic bomb at Hiroshima at 1–1.5 km distance from ground zero (2). At this distance, both survival and radiation exposure are expected to be sufficiently high to require triage for allocation of medical efforts; based on the Hiroshima data, most survivors around this distance receive an appreciable neutron dose [up to 0.25 Gy (4)]. However, the spectrum observed at this distance is significantly different from a standard reactor spectrum due to transport in the air, and has a larger component of low-energy neutrons. It is expected that this difference would have a significant impact on biodosimetric dose reconstruction.

The neutron field is produced by a mixed beam, composed of 5 MeV atomic and molecular ions of hydrogen and deuterium, which is used to bombard a thick beryllium (Be) target. Beryllium is a well-known neutron-producing material not only because of its high neutron yield but also because of its stability and high specific heat. This mixed beam produces a neutron spectrum, which is the sum of the spectra from the  ${}^9\text{Be}(d,n){}^{10}\text{B}$  and  ${}^9\text{Be}(p,n){}^9\text{B}$  reactions for all the incident ions (monatomic, diatomic and triatomic) and for energies from 5 MeV and down. In general, for monatomic 5 MeV projectiles, the  ${}^9\text{Be}(d,n){}^{10}\text{B}$  reaction provides a spectrum with higher energy neutrons (above 1 MeV) while the  ${}^9\text{Be}(p,n){}^9\text{B}$  reaction primarily yields neutrons below 1 MeV. These nuclear reactions generate a combined neutron spectrum with a wide range of energies, which can then be used to irradiate biological samples and small animals (e.g., mice) for radiobiology studies. The

<sup>1</sup> Scholar in training.

<sup>2</sup> Address for correspondence: Columbia University, Radiological Research Accelerator Facility, 136 S. Broadway, P.O. Box 21, Irvington, NY 10533; email: gyg2101@cumc.columbia.edu.

beam composition in the current setup is approximately a 1:2 ratio of protons to deuterons. However, for other scenarios, the spectrum shape can be modified by adjusting the ratio of protons to deuterons and the incident beam energy.

As described elsewhere (5), the neutron spectra were evaluated by making combined measurements with a proton-recoil proportional counter (6) and liquid scintillator detector (7). The measured recoil spectra were unfolded using maximum entropy deconvolution (8), based on Monte Carlo simulated detector response functions (9).

The dosimetry for the irradiations was performed using a custom tissue-equivalent (TE) gas ionization chamber, placed on the sample holder wheel. This chamber measures the total dose in the mixed neutron and gamma-ray field. To evaluate the ratio of neutron and gamma doses, gamma-ray dosimetry was performed separately by replacing the ionization chamber with a compensated Geiger-Mueller dosimeter, which has a very low neutron response (10). These measurements indicated that all neutron exposures using this spectrum are accompanied by a parasitic photon dose of about 21% of the total dose delivered.

To account for possible variations in the dose rate during radiation exposures, a second TE gas ionization chamber was placed in a fixed location on the beam axis, directly downstream of the neutron target and used as a monitor. All measurements were normalized to the signal from the monitor, which is used to determine the dose during irradiation.

In a realistic scenario it is expected that the neutron dose would be only a small fraction of the total exposure [e.g., DS02 reported only 2% neutron dose at 1.5 km from the Hiroshima epicenter (4)]. To mimic such a mixed field, a 250 kVp orthovoltage X-ray machine is located on site, which allows irradiation of samples with the necessary additional dose of photons.

To demonstrate the use of this facility, we show results from initial tests using the *in vitro* cytokinesis-block micronucleus assay (CBMN) (11) to measure the induction of micronuclei in peripheral human blood lymphocytes exposed to a range of neutron doses up to 1.5 Gy. The dose-response curves generated for micronuclei frequency indicated that the relative biological effectiveness (RBE) of this neutron spectrum is between 3 and 5 compared to micronucleus yields induced by 250 kVp X rays. As expected, these values fall between those for accelerator-generated energetic neutrons (12) and those for a reactor-based uranium fission spectrum (12, 13).

## FORMATION OF A BROAD NEUTRON SPECTRUM

The key feature of our broad-energy neutron irradiator is its use of a mixed gas ion source, with the spectrum depending on the ratio of gases in the mixture fed into the ion source. For this work, hydrogen and deuterium were combined at a ratio of 1:2 in one of the ion source gas

supply cylinders and placed in the accelerator terminal. The ionization process of the mixed gas is complicated, as it generates many different ion combinations. To identify the actual ion beam ratios and to optimize the beam current, two different values of the gas valve control voltage were tested. The selected gas input parameter (percentage of maximum valve voltage) is used to control the pressure and provide sufficient beam current. To determine the ratio of the different ion species in our beam we measured beam current at a 15° deflection as a function of the field strength of the bending magnet. Table 1 shows the fractions of the various atomic and molecular ions at two extremal pressures we can use (outside this pressure range, the beam current is too low or the ion source operation is unstable). Several ion species (e.g.,  $D^+$  and  $H_2^+$ ) cannot be separated magnetically because their magnetic rigidity is very close. As can be seen, increasing the valve voltage from 65.2 to 76.6% changed the ion ratios slightly for the molecular ions, but not atomic ions. As the major contributions to the spectrum come from the  $H^+$  and  $D^+$  ions, which vary by less than 2% over this range, we expect the spectrum will not vary significantly over this range of ion source parameters.

Neutrons are generated as the particle beam impinges on a thick (500  $\mu\text{m}$ ) beryllium target. At this thickness, the 5 MeV deuterons and protons are completely stopped in the beryllium. The neutron energy spectrum obtained by this configuration was previously (3) modeled using MCNPX and more recently validated experimentally (5). Briefly, an EJ-301 liquid-filled scintillation detector and a gas proportional counter filled with 3 atm of hydrogen were used for measuring neutron energies above and below 1.0 MeV, respectively. The combination of the two detection systems covers a wide energy range, from 0.2 to >9 MeV. The recoil pulse height spectra acquired by the detector systems were carefully evaluated using different quasi-monoenergetic neutron beams (0.2–9 MeV) available at the RARAF accelerator, discriminating the gamma-ray signals from the raw acquisition data with pulse rise time (5).

The two portions of the spectrum (obtained from the two detectors) were combined to form a kerma-weighted total spectrum (Fig. 1). Overall, the obtained spectrum is similar to the one evaluated for Hiroshima (2), although it is slightly flatter. A more detailed discussion of the differences between our spectrum and Hiroshima has been reported elsewhere (5).

## IRRADIATION SETUP

Due to the requirement for a mixed hydrogen/deuterium beam, the irradiation facility was set up using a non-deflected (0° angle) beam line in the RARAF (Fig. 2A). The target assembly, shown in Fig. 2B, consists of a 2 mm thick, copper disk onto which a 500  $\mu\text{m}$  thick beryllium foil was diffusion bonded. The dimensions of the copper disk were chosen so that it can be used in lieu of a standard

**TABLE 1**  
**Ion Species Percentage for Two Different Percentages**  
**of Maximum Gas Control Voltage**

Gas valve setting	65.2%	76.6%
Ion species		
D <sup>+</sup> , H <sub>2</sub> <sup>+</sup>	35.75%	37.3%
D <sub>2</sub> <sup>+</sup> , H <sub>2</sub> D <sup>+</sup>	25.1%	16.7%
D <sub>3</sub> <sup>+</sup>	7.26 %	12%
H <sup>+</sup>	15%	16%
H <sub>3</sub> <sup>+</sup>	7.8%	2.2%
D <sub>2</sub> H <sup>+</sup>	8.9%	16%
Total current	1.8 μA	1.5 μA

2.75" Conflat gasket. The target is clamped between two Conflat flanges and doubles as a vacuum window. The target is cooled by water impinging on the copper backing plate (3).

Since the target cooling water lines, supporting structures, shielding and other surrounding materials were observed to give about a 20% azimuthal variation in dose rate, a vertical Ferris wheel-like fixture (Fig. 2A) was used to rotate the sample holder tubes (for either blood or mice) around the target. Customized tubes mounting from the rods on the wheel were used to hold the samples with a constant horizontal orientation at a distance of 190 mm from the target center. The fixture rotates up to 18 samples around the beam axis. The sample holders for both mice and *ex vivo* irradiated blood are based on standard 50 ml conical centrifuge tubes (BD Diagnostics, Franklin Lakes, NJ), which were modified to enable horizontal hanging from rods on the wheel, so that the tubes maintain a constant horizontal orientation as the wheel rotates. This provides an isotropic irradiation, while maintaining the mice in an upright orientation, reducing stress. During irradiations, the speed of the Ferris wheel is about one rotation per 2 min and the dose rate adjusted so that the minimal dose is delivered in 10 rotations (20 min), and the sample tubes are flipped end-to-end halfway through the process so that the front and back of each sample receives equivalent doses.

For pure photon exposures, a 250 kVp Westinghouse Coronado X-ray machine, located within 15 m of the neutron irradiation facility, was used. This proximity allows for future mixed field studies, where each sample may be immediately transported to the X-ray machine and irradiated after neutron exposure, with a time gap between the two irradiations of less than 5 min.

### NEUTRON DOSIMETRY

The total dose measurement for the IND-like neutron/gamma mixed field irradiations was performed using a custom A-150 muscle tissue-equivalent (TE) gas ionization chamber (Fig. 3), as described by Rossi *et al.* (14). This chamber is intended for use in a mixed neutron- and

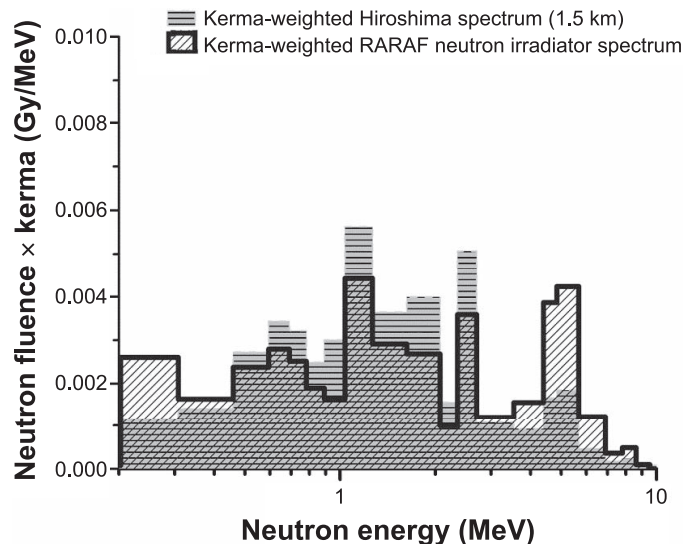


**FIG. 1.** A comparison of the kerma-weighted neutron spectrum generated by the authors for this study (hashed) with the one at 1.5 km from Hiroshima ground zero (gray) (2).

gamma-field measurement and features an interchangeable internal TE plastic sleeve. In the dosimetry measurements reported here, we used a 3.5 mm thick sleeve to model the dose deposited at the center of the blood samples used. The chamber was filled with methane TE gas at ~700 mm Hg before dosimetry measurement and sealed. The detector was then attached directly to an electrometer system and calibrated using a 50 mg <sup>226</sup>Ra gamma-ray source, which had been previously calibrated by the National Institute of Standards and Technology. The dose rate was ~36 μGy/h at 1 m from the source. After calibration, the dosimeter was mounted on the sample wheel for the IND-like neutron irradiator and centered at 60° with respect to the ion beam axis and 190 mm away from the target.

To extract the dose due to neutrons, gamma-ray dosimetry was performed separately with a compensated Geiger-Mueller dosimeter, which has a neutron sensitivity of 1.5% for 15 MeV neutrons and a fraction of a percent at lower energies (10, 15). The gamma-ray dosimetry was conducted in the same manner as the total dose measurement and then subtracted from the latter. Since the gamma-ray dose from the target is essentially isotropic, only inverse square law corrections were performed.

The neutron dose rate at the sample position was ~8.6 × 10<sup>-2</sup> Gy/h/μA, representing ~79% of the total dose rate, with the remaining 21% due to γ rays. During the irradiation, the beam current was tuned to and kept at about 17.5 μA, which is equal to a neutron dose rate of ~1.5 Gy/h.

Because of the possible variation of the dose rate relative to the beam current, a second TE gas ionization chamber was added as a monitor at a fixed location downstream of

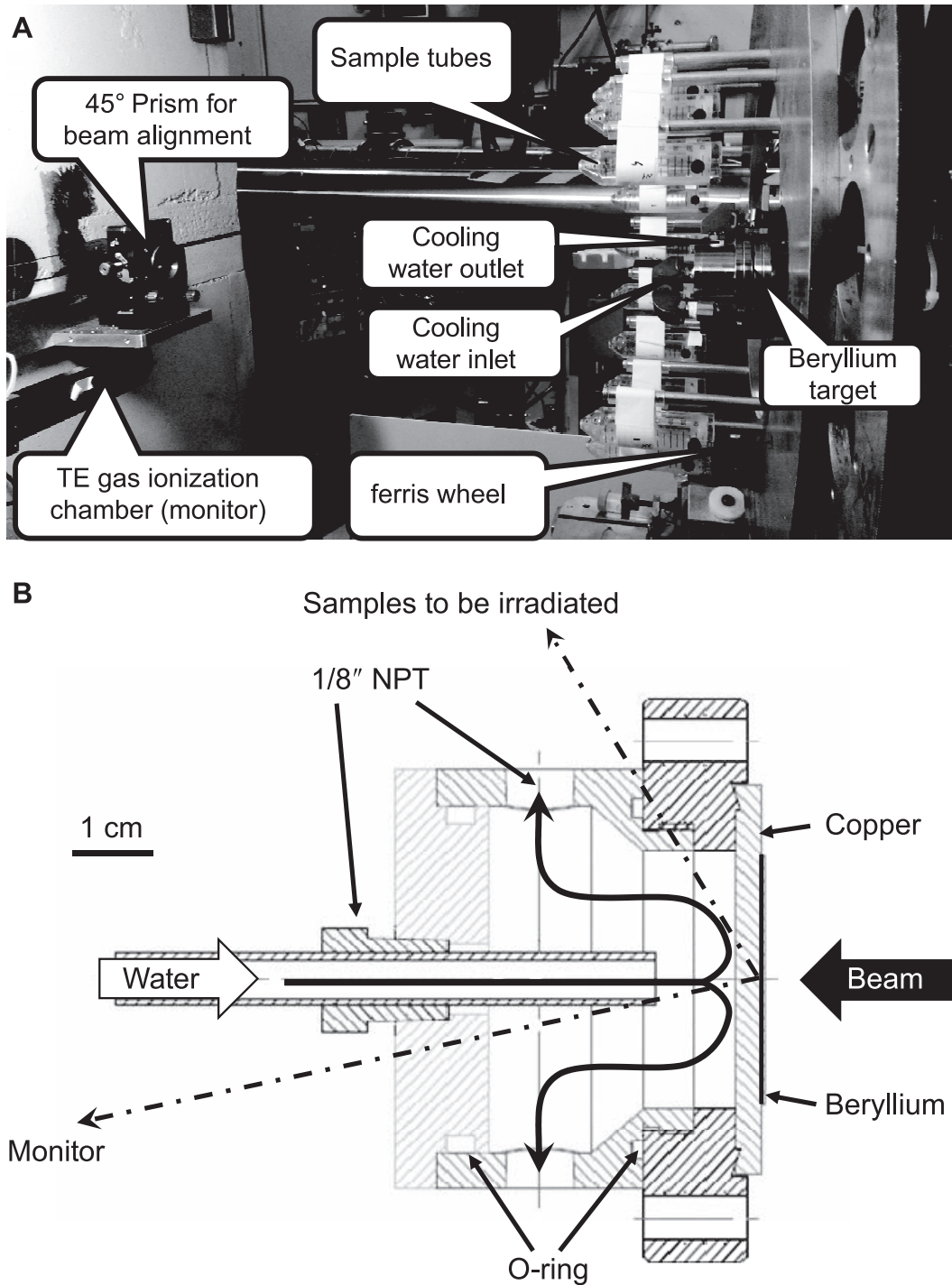


**FIG. 2.** Panel A: Photo of the irradiation facility. Beam arrives from the right and impinges on the beryllium target generating neutrons. Samples to be irradiated (blood or mice) are placed in sample holders (shown here empty) and mounted on a Ferris wheel rotating around the target-cooling chamber. At the left is the tissue-equivalent gas ionization chamber used as a beam monitor and the right angle prism used for aligning the beam line. Panel B: Cross section of target and cooling chamber. Direction to the center of the sample holders (190 mm away) and the monitor chamber (610 mm away) are shown.

the neutron target at an angle of  $\sim 12^\circ$  relative to the ion beam direction. The monitor ionization chamber was filled with flowing TE gas, which was regulated with a constant-density control system.

The incident primary particle beam current was recorded with an electrometer coupled to the end of the beam line, which is a Faraday cup-like isolated beam pipe with the target at the end.

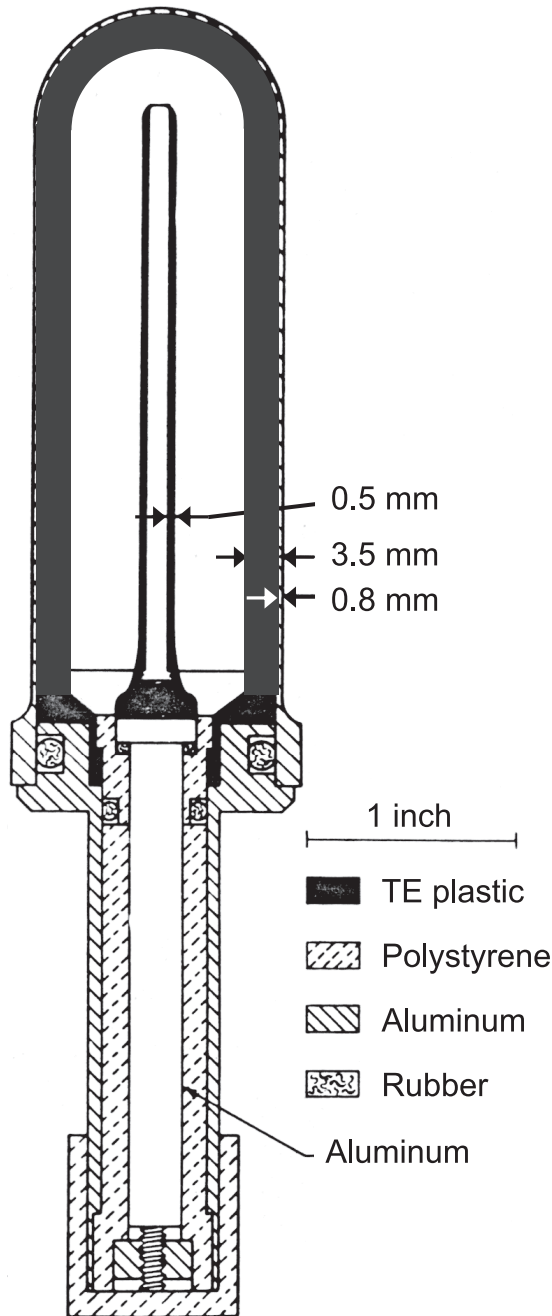


**FIG. 3.** Custom tissue-equivalent gas ionization chamber for neutron dosimetry, shown here with 3.5 mm thick tissue-equivalent plastic sleeve. This figure was originally published by Rossi *et al.* "The dependence of RBE on the energy of fast neutrons: 1. Physical design and measurement of absorbed dose." *Radiat Res* 1960; 13:503–20 (14), modified and republished with the permission of *Radiation Research*.

### MICRONUCLEUS ASSAY ANALYSIS

Micronucleus formation in peripheral blood lymphocytes is a well-established marker of ionizing radiation-induced DNA damage. We have used a recently established cytokinesis-block micronucleus (CBMN) assay protocol by Fenech (11) for accelerated sample processing by

performing a miniaturized version of the assay in a 96-well plate system (16).

Peripheral blood samples were collected from three healthy donors after informed consent (IRB protocol no. AAAF2671) and exposed (3 ml aliquots) to nominal neutron doses of approximately 0.25, 0.5, 1 and 1.5 Gy (plus the concomitant 0.06, 0.1, 0.2 and 0.3 Gy of gamma rays). Separate blood sample aliquots were also exposed to 1, 2 and 4 Gy of 250 kVp X rays.

During irradiation, between 3 and 12 tubes were placed in adjacent positions on the irradiation wheel. To ensure a uniform scatter dose, 4 tubes containing water samples were placed on the wheel, two at either end of the string of blood samples. Approximately 2 h postirradiation, triplicate blood sample aliquots (50  $\mu$ l) from each dose point were placed into culture in 1.0 ml Matrix 2D-barcode storage tubes (Thermo Fisher Scientific, Waltham, MA) with 500  $\mu$ l of PB-MAX™ Karyotyping media (Life Technologies, Grand Island, NY). After 44 h of incubation, cytochalasin B (Sigma-Aldrich LLC, St. Louis, MO) was added at a final concentration of 6  $\mu$ g/ml to inhibit cell cytokinesis and the tubes were returned to the incubator. After a total incubation period of 72 h, the cells were harvested. After hypotonic treatment the cells were fixed with ice-cold fixative (4:1 methanol:acetic acid). The fixed samples were stored at 4°C (at least overnight), dropped on slides and stained with Vectashield® mounting media containing DAPI (Vector Laboratories, Burlingame, CA). The slides were imaged using a Zeiss fluorescence microscope (Axioplan 2; Carl Zeiss MicroImaging Inc., Thornwood, NY) with a motorized stage and a 10 $\times$  air objective. Quantification of lymphocyte micronuclei yields was performed by automatic scanning and analysis with the MetaferMN Score software (MetaSystems, Althausen, Germany). Between 1,800 and 6,000 binucleate cells were analyzed for each data point.

Figure 4A shows the comparison of the micronucleus yields for lymphocytes exposed to different neutron or X-ray doses. Overall, a dose-dependent increase in micronuclei yields was observed with increasing dose with both radiation fields, with the yields induced by the X rays following a linear-quadratic behavior with dose and the neutron data following a linear trend.

As explained above, the neutron data are actually induced by a mixed neutron/photon field. The dashed line shown in Fig. 4A illustrates what we would expect from a pure neutron irradiation. This estimate was obtained by calculating excess micronucleus yields over controls from the photon component (21% of the total dose) based on the linear-quadratic fit to the X-ray data. This value was then subtracted from the mixed field yields at the same total dose. The resultant difference corresponds to the micronuclei yields that would be seen in a pure neutron irradiation.



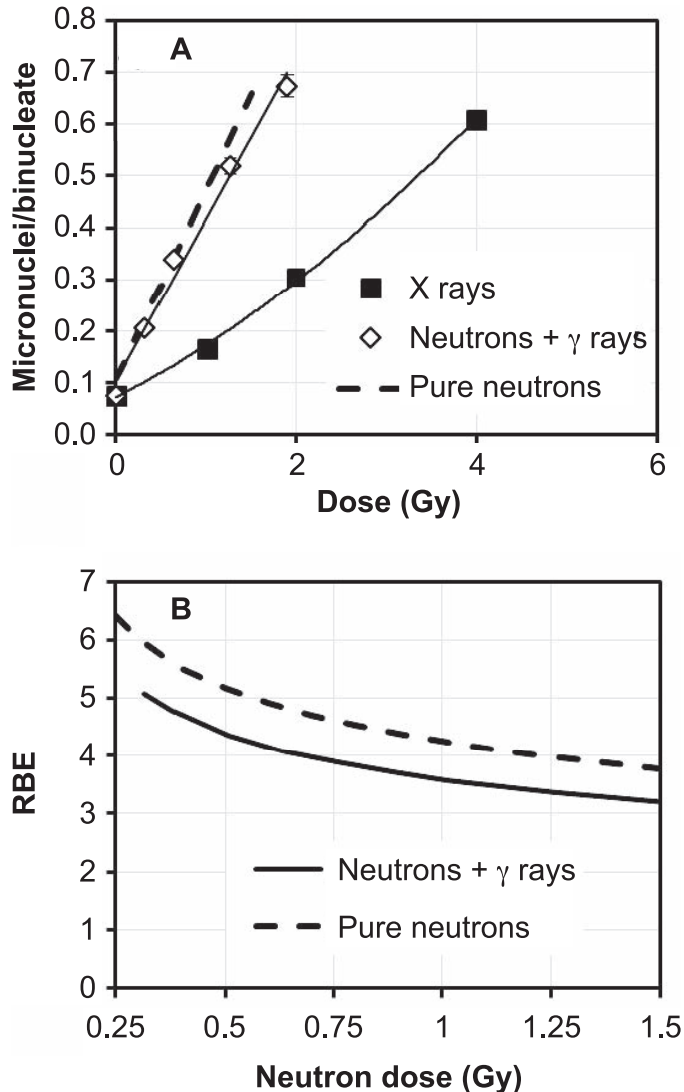


**FIG. 4.** Panel A: Micronucleus frequency in human peripheral blood lymphocytes exposed *ex vivo* to neutrons or X rays. The data show mean micronuclei per binucleate cell yields from three healthy volunteers. Error bars show  $\pm$ SEM. The mixed field yields plotted vs. total dose (neutrons + gamma rays). The solid lines indicate a linear (neutrons) or linear-quadratic (X rays) fit. The dashed line indicates the estimated response to a pure neutron dose. Panel B: RBE values for the mixed field and for the pure neutrons, calculated from panel A (see text for details).

#### RELATIVE BIOLOGICAL EFFECTIVENESS CALCULATIONS

The potential biological effects and damage caused by radiation depend not only on the radiation dose received but also on the type of radiation. RBE was introduced to normalize the radiobiological effects caused by different types of radiation. In this work, we define RBE as the ratio of photon dose (250 kVp X rays) to the dose of the radiation field of interest (neutrons), providing the same biological effect (17). The biological effects caused by neutrons vary with energy and produce greater damage than X or gamma

rays. In general, for the same dose, neutrons are much more effective in damaging cells because neutron-induced secondary particles, e.g., low-energy protons, have high-LET (linear energy transfer) and photon-induced particles are electrons having low LET.

The RBE for the mixed field irradiation (neutrons + gamma rays; Fig. 4B) was calculated from the linear and linear-quadratic regression curves, fitted to the neutron and X-ray data, respectively, by solving for the X-ray dose that would give the same micronucleus yield as a given dose of the mixed neutron/gamma-ray field. The pure neutron RBE will be slightly higher than the RBE value of the mixed field. This was evaluated in the same way from the dashed line shown in Fig. 4A.

Figure 4B shows the limiting RBE value of 4 is higher than the value of 2.5 reported for 6 MeV monoenergetic neutrons (12) but lower than the value of 6 calculated for a reactor fission spectrum (13), in accordance with what we would expect, based on the neutron energies.

#### SUMMARY

An accelerator-based, broad-energy-range neutron irradiator has been constructed at RARAF. A mixed beam of atomic and molecular deuterons and protons, accelerated to 5 MeV, impinges on a thick beryllium target and the resultant neutron spectrum is the sum of the spectra from the  ${}^9\text{Be}(d,n){}^{10}\text{B}$  reaction (higher energy neutrons) and the  ${}^9\text{Be}(p,n){}^9\text{B}$  reaction (lower energy neutrons). The neutron energy spectrum is manipulated by adjusting the ratio of protons and deuterons, as well as the beam energy, to mimic the neutron spectra from an IND exposure for medical triage and biodosimetry studies. Specifically, it mimics the Hiroshima gun-type bomb spectrum at a relevant distance from the epicenter (1–1.5 km) and is significantly different from a standard reactor fission spectrum because the bomb spectrum changes as the neutrons are transported through air. The neutron spectrum of this irradiator was measured and is verified as comparable to the Hiroshima bomb spectrum at 1.5 km. About 79% of the radiation dose is delivered by neutrons and the remaining dose delivered by gamma rays. A comparison of the biological effect of neutron and X-ray exposure on micronuclei yields in peripheral lymphocytes demonstrated that the IND-spectrum irradiator described above yields RBE values within the expected range.

The RBE measurements described here have demonstrated the operation of the novel neutron irradiation facility we have developed. Ongoing experiments at the RARAF IND-neutron irradiation facility focus on dose reconstruction in mixed neutron/photon radiation fields using various cytogenetic end points. Additional experiments, using metabolomic and transcriptomic end points, are aimed at a more basic understanding of the underlying pathways activated after neutron irradiation.

## ACKNOWLEDGMENTS

This work was supported by a grant to the Center for High-Throughput Minimally Invasive Radiation Biodosimetry from the National Institute of Allergy and Infectious Diseases (NIAID), National Institutes of Health (NIH), grant no. U19-AI067773. The content is solely the responsibility of the authors and does not necessarily represent the official views of the NIAID or NIH. The authors would like to acknowledge the continued support of Gary Johnson from the Design and Instrument Shop at the Center for Radiological Research, Columbia University Medical Center. Without him, this work would not be possible. Some of the reagents and plastic ware used in this work were purchased through Fisher Scientific. At the time of writing this manuscript GG owns 90 shares of Thermo Fisher Scientific stock.

Received: February 1, 2015; accepted: August 4, 2015; published online: September 28, 2015

## REFERENCES

1. National planning scenarios (final version 21.3). Washington, DC: Homeland Security Council; 2006. (<http://1.usa.gov/1gGvsQ7>)
2. Egbert SD, Kerr GD, Cullings HM. DS02 fluence spectra for neutrons and gamma rays at Hiroshima and Nagasaki with fluence-to-kerma coefficients and transmission factors for sample measurements. *Radiat Environ Biophys* 2007; 46:311–25.
3. Xu Y, Garty G, Marino SA, Massey TN, Randers-Pehrson G, Johnson GW, et al. Novel neutron sources at the Radiological Research Accelerator Facility. *J Instrum* 2012; 7:C03031.
4. Young RW, Egbert SD, Cullings HM, Kerr GD, Imanaka T. Survivor dosimetry part B. DS02 free-in-air neutron and gamma tissue kerma relative to DS86. In: Young RW, Kerr GD, editors. Reassessment of the atomic bomb radiation dosimetry for Hiroshima and Nagasaki: dosimetry system 2002. Hiroshima, Japan: Radiation Effects Research Foundation; 2005.
5. Xu Y, Randers-Pehrson G, Marino S, Garty G, Brenner D. Broad energy range neutron spectroscopy with a liquid scintillator and a proportional counter: application to a neutron spectrum similar to that from an improvised nuclear device. *Nucl Instr Meth A* 2015; 794:234–9.
6. Tagziria H, Hansen W. Neutron spectrometry in mixed fields: proportional counter spectrometers. *Radiat Prot Dosimetry* 2003; 107:73–93.
7. Klein H. Neutron spectrometry in mixed fields: NE213/BC501A liquid scintillation spectrometers. *Radiat Prot Dosimetry* 2003; 107:95–109.
8. Reginatto M, Goldhagen P, Neumann S. Spectrum unfolding, sensitivity analysis and propagation of uncertainties with the maximum entropy deconvolution code MAXED. *Nucl Instr Meth A* 2002; 476:242–6.
9. Pozzi SA, Flaska M, Enqvist A, Pázsit I. Monte Carlo and analytical models of neutron detection with organic scintillation detectors. *Nucl Instr Meth A* 2007; 582:629–37.
10. Wagner EB, Hurst GS. A Geiger-Mueller  $\gamma$ -ray dosimeter with low neutron sensitivity. *Health Phys* 1961; 5:20–6.
11. Fenech M. Cytokinesis-block micronucleus cytome assay. *Nat Protoc* 2007; 2:1084–104.
12. Wuttke K, Müller W-U, Streffer C. The sensitivity of the in vitro cytokinesis-blocked micronucleus assay in lymphocytes for different and combined radiation qualities. *Strahlenther Onkol* 1998; 174:262–8.
13. Huber R, Schraube H, Nahrstedt U, Braselmann H, Bauchinger M. Dose-response relationships of micronuclei in human lymphocytes induced by fission neutrons and by low LET radiations. *Mutat Res* 1994; 306:135–41.
14. Rossi HH, Bateman JL, Bond VP, Goodman LJ, Stickley EE. The dependence of RBE on the energy of fast neutrons: 1. Physical design and measurement of absorbed dose. *Radiat Res* 1960; 13:503–20.
15. An international neutron dosimetry intercomparison. ICRU Report No. 27. Washington, DC: International Commission on Radiation Units and Measurements; 1978.
16. Lue S, Repin M, Mahnke R, Brenner D. Development of a high-throughput and miniaturized cytokinesis-block micronucleus assay for use as a biological dosimetry population triage tool. *Radiat Res* 2015; 184:134–42.
17. Hall EJ, Giaccia AJ. *Radiobiology for the radiologist*. 7th ed. Philadelphia: Lippincott, Williams & Wilkins; 2012.